RESEARCH PAPER

Quality-by-Design-Driven Optimization of Tofacitinib Nanocrystals: Influence of Pluronic F127 and Sonication on Critical Quality Attributes

SWAPNA PAUL[1], DR. VIVEK CHAUHAN[2]

[1]Research Scholar, SHRI JAGDISH PRASAD JHABARMAL TIBREWALA UNIVERSITY, VIDYANAGARI, JHUNJHUNU, RAJASTHAN – 333001.
Assistant Professor, St. James college of Pharmaceutical Sciences, Chalakudy.

[2]Professor SHRI JAGDISH PRASAD JHABARMAL TIBREWALA UNIVERSITY, VIDYANAGARI, JHUNJHUNU, RAJASTHAN – 333001

Main Corresponding Author: Swapna Paul (Email id : swapnapaulrosna@gmail.com)

Abstract

Background: Tofacitinib is a poorly water-soluble drug, and its limited dissolution may restrict oral bioavailability. This study aimed to develop and optimize Tofacitinib nanocrystals using Pluronic F127 and sonication to enhance dissolution performance.

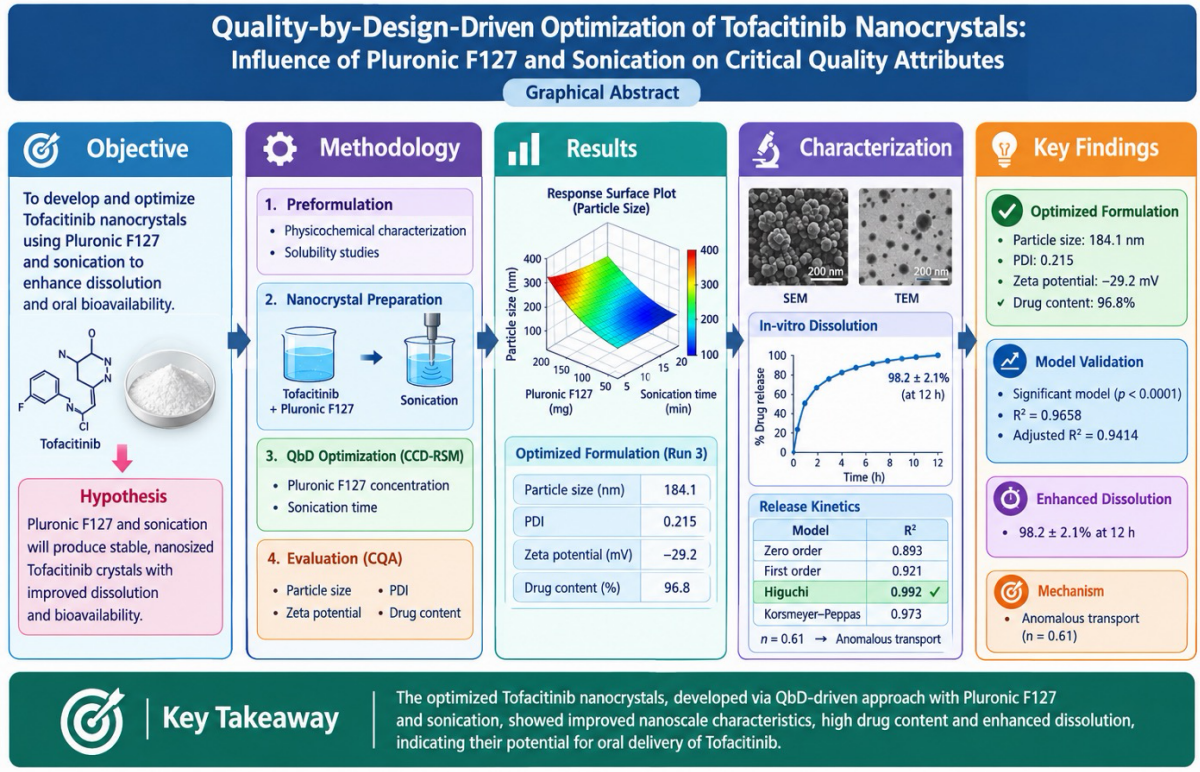
Methods: Preformulation studies were conducted to establish the physicochemical characteristics and solubility of Tofacitinib. Nanocrystals were prepared using Pluronic F127 as a stabilizer and optimized using Central Composite Design (CCD)-based Response Surface Methodology (RSM). Pluronic F127 concentration and sonication time were selected as critical formulation variables, while particle size, polydispersity index (PDI), zeta potential, and drug content were evaluated as responses. The optimized formulation was characterized by SEM, TEM, and *in-vitro* dissolution studies. Drug-release data were fitted to different kinetic models.

Results: The optimized formulation (Run 3) exhibited a particle size of 184.1 nm, PDI of 0.215, zeta potential of −29.2 mV, and drug content of 96.8%. Across the formulations, these responses ranged from 184.1–389.7 nm, 0.214–0.468, −14.8 to −29.2 mV, and 79.8–96.8%, respectively. The quadratic model was significant ($p < 0.0001$; $R^2 = 0.9658$; adjusted $R^2 = 0.9414$) and demonstrated the significant effects of Pluronic F127 and sonication time. SEM and TEM confirmed discrete, uniformly distributed nanocrystals with minimal aggregation. The optimized formulation achieved 98.2 ± 2.1% drug release at 12 h. Release kinetics showed the best fit to the Higuchi model ($R^2 = 0.992$), with a Korsmeyer–Peppas *n* value of 0.61, indicating anomalous transport.

Conclusion: The optimized Tofacitinib nanocrystals demonstrated improved nanoscale characteristics, high drug content, and enhanced dissolution, indicating their potential as a promising strategy for improving the oral delivery of Tofacitinib.

Keywords: Tofacitinib; Nanocrystals; Pluronic F127; Sonication; Central Composite Design; Quality by Design; Response Surface Methodology.

How to cite this article: SWAPNA PAUL1 DR. VIVEK CHAUHAN2. Quality-by-Design-Driven Optimization of Tofacitinib Nanocrystals: Influence of Pluronic F127 and Sonication on Critical Quality Attributes. Int J Drug Deliv Technol. 2026;16(90s):1359-1372. DOI: 10.25258/ijddt.16.90s.135.



Introduction

Tofacitinib is a small-molecule Janus kinase inhibitor widely used for the treatment of inflammatory and autoimmune disorders; however, its formulation performance can be influenced by its physicochemical and biopharmaceutical properties [1]. Poor aqueous solubility represents a major formulation challenge because inadequate dissolution may limit drug availability and therapeutic performance [2]. Drug nanocrystals offer an attractive strategy for poorly water-soluble drugs, as nanosizing increases specific surface area and can enhance dissolution and apparent solubility [3]. However, suitable polymeric or surfactant stabilizers are generally required to minimize aggregation and crystal growth and maintain nanoscale characteristics [4]. Pluronic F127, an amphiphilic triblock copolymer, has been extensively investigated as a pharmaceutical excipient and stabilizer in nanoscale drug-delivery systems [5]. High-energy sonication can facilitate particle-size reduction during nanocrystal preparation, although its processing conditions require careful control to obtain reproducible nanosized particles [6]. https://pubmed.ncbi.nlm.nih.gov/38299478/?utm_source=chatgpt.com Recent research on tofacitinib nanoformulations has demonstrated that nanoscale formulation combined with systematic experimental optimization can produce desirable particle characteristics and improved drug-release performance [7]. Quality-by-Design (QbD) and Design of Experiments (DoE) provide a systematic framework for identifying critical formulation variables and their interactions rather than relying on conventional one-factor-at-a-time experimentation [8]. Central Composite Design (CCD) combined with Response Surface Methodology (RSM) is particularly useful for developing predictive quadratic models and identifying optimized formulation conditions [9]. However, the systematic optimization of tofacitinib nanocrystals using Pluronic F127 concentration and sonication time as critical formulation and process variables remains insufficiently investigated [10]. Therefore, the present study aimed to develop and optimize tofacitinib nanocrystals using Pluronic F127 and sonication through a QbD-driven CCD/RSM approach, followed by physicochemical characterization and evaluation of dissolution performance.

Materials and Methods

Tofacitinib was procured from Swarnoop Pharmaceuticals, India. Pluronic F127 was purchased from [Sigma-Aldrich/Merck, India]. Distilled water was used as the dispersion medium and for all experimental procedures. All other chemicals and reagents used in the study were of analytical grade and were obtained from standard commercial suppliers.

Materials

Solubility Study

The equilibrium solubility of Tofacitinib was determined in distilled water, deionized water, 0.1 N HCl, phosphate buffers (pH 6.8 and 7.4), methanol, ethanol, acetone, N, N-dimethylacetamide (DMAc), and dimethyl sulfoxide (DMSO). Excess drug (50–100 mg) was added to 10 mL of each solvent in sealed glass vials and equilibrated at 25 ± 2 °C for 48 h under orbital shaking (100 rpm). The samples were centrifuged at 5000 rpm for 10 min and the supernatants were filtered through 0.45 µm membrane filters. After suitable dilution, Tofacitinib concentration was quantified at 287 nm using UV–visible spectrophotometry and expressed as mg/mL. Measurements were performed in triplicate and reported as mean ± SD. DMSO was selected as the organic solvent based on its superior solubilizing capacity. The poor aqueous solubility of Tofacitinib supports the application of nanotechnology-based approaches to improve its aqueous dispersion and delivery [11].

Melting Point Determination

The melting point of Tofacitinib was determined by the capillary method using finely powdered drug packed to approximately 2–3 mm height. The temperature was increased at 1–2 °C/min near the expected melting range, and the onset and completion of melting were recorded. The analysis was performed in triplicate and the mean value was compared with reported literature data. Thermal behavior was further evaluated by DSC using 3–5 mg of drug in sealed aluminium pans, with an empty pan as reference. Samples were heated from 30 to 300 °C at 10 °C/min under nitrogen purge, and the characteristic endothermic transition was recorded. DSC has been used to characterize the solid-state and thermal behavior of Tofacitinib and its pharmaceutical forms [12].

FTIR Compatibility Study

FTIR spectroscopy was performed to evaluate drug–excipient compatibility and structural changes following nanocrystal preparation. Tofacitinib, Pluronic F127, their physical mixture, and the optimized nanocrystals were dried for 24 h and scanned over 4000–400 cm^{-1} at a resolution of 4 cm^{-1} using 16–32 scans. The characteristic absorption bands of Tofacitinib were compared among the samples. Retention of the principal drug bands without significant shifts, disappearance of characteristic peaks, or appearance of new bands was considered indicative of the absence of major chemical interactions. FTIR characterization has similarly been employed for Tofacitinib-containing formulations to assess drug–excipient compatibility and preservation of characteristic functional groups [13].

Methodology and Optimization

Tofacitinib nanocrystals will be prepared by antisolvent precipitation followed by probe sonication. Tofacitinib (100 mg) will be dissolved in acetone (10 mL), while Pluronic F127 will be dispersed in distilled water (50 mL). The drug solution will be added dropwise (1 mL/min) into the aqueous stabilizer phase under continuous stirring (1200 rpm), followed by probe sonication at 40% amplitude using a pulse mode (5 s ON/3 s OFF).

Optimization will be performed using Response Surface Methodology–Central Composite Design (RSM-CCD). The independent variables will be X_1: drug: Pluronic F127 ratio (1:0.3–1:1.7) and X_2: sonication time (3–17 min). The dependent responses will be Y_1: particle size, Y_2: PDI, Y_3: zeta potential and Y_4: drug content. Particle size and PDI will be minimized, whereas zeta potential and drug content will be maximized. The optimized formulation will be selected based on minimum particle size (<250 nm), PDI (<0.30), adequate zeta potential (≥±20 mV) and drug content (>90%). Quadratic models, ANOVA, contour plots and three-dimensional response-surface plots will be used to establish the optimized formulation [9,10,14].

Table 1. Consolidated Optimization Design with Factor Levels for Tofacitinib Nanocrystals

Optimization Parameter	Code	Unit	−α	−1 (Low)	0 (Center)	+1 (High)	+α
Drug: Pluronic F127 ratio	X_1	Ratio	1:0.3	1:0.5	1:1.0	1:1.5	1:1.7
Pluronic F127	X_1	mg/100 mg drug	30	50	100	150	170
Pluronic F127	—	% w/v	0.06	0.10	0.20	0.30	0.34
Sonication time	X_2	min	3	5	10	15	17

Folic Acid Functionalization

The optimized nanocrystals will be surface-functionalized with folic acid using EDC/NHS coupling. Folic acid (10–20 mg) will be activated with equimolar EDC/NHS for 30–60 min and added to the optimized Pluronic-coated nanocrystals under stirring (500–700 rpm) for 6–12 h. The functionalized nanocrystals will be purified by centrifugation (15,000 rpm, 20 min), washed and redispersed or freeze-dried for further characterization [15-25].

Dynamic Light Scattering (DLS) Analysis

Dynamic light scattering (DLS) was used to determine the hydrodynamic particle size, polydispersity index (PDI), and zeta potential of the prepared Tofacitinib nanocrystals. The nanocrystal dispersion was appropriately diluted with filtered deionized water, gently mixed, and analyzed at 25 °C using a laser-based particle-size analyser. Particle size and PDI were measured in a disposable cuvette, while zeta potential was determined using an electrophoretic cell. A nanoscale particle size with a narrow, preferably unimodal distribution and low PDI indicated successful nanosizing, whereas zeta potential was used to assess colloidal stability.

Table 2: Central Composite Design (CCD) – for optimization of Nanocrystal formulation

Run	X_1 Level	Drug: Pluronic F127 Ratio	Pluronic F127 (mg)	Concentration in 50 mL Water (% w/v)	X_2 Level	Sonication Time (min)
1	-1	100:50	50 mg	0.10%	-1	5
2	+1	100:150	150 mg	0.30%	-1	5
3	-1	100:50	50 mg	0.10%	+1	15
4	+1	100:150	150 mg	0.30%	+1	15
5	-α	100:30	30 mg	0.06%	0	10
6	+α	100:170	170 mg	0.34%	0	10
7	0	100:100	100 mg	0.20%	-α	3
8	0	100:100	100 mg	0.20%	+α	17
9	0	100:100	100 mg	0.20%	0	10
10	0	100:100	100 mg	0.20%	0	10
11	0	100:100	100 mg	0.20%	0	10
12	0	100:100	100 mg	0.20%	0	10
13	0	100:100	100 mg	0.20%	0	10

X_1 = drug: Pluronic F127 ratio; X_2 = sonication time. F127 concentration was calculated for 50 mL aqueous phase. Runs 9–13 are center-point replicates for estimating experimental error.

A. Particle Size

The mean hydrodynamic particle size of the Tofacitinib nanocrystals was determined by DLS based on Brownian motion of dispersed particles. Particle size is a critical quality attribute influencing dissolution, physical stability, and drug-release behaviour. The optimized formulation was targeted to obtain a nanoscale particle size (<250 nm), facilitating increased surface area and improved dissolution of the poorly water-soluble drug [26,27].

B. Polydispersity Index (PDI)

PDI was determined by DLS to assess the uniformity of particle-size distribution. Lower PDI values indicate a more homogeneous particle population, whereas higher values suggest broader size distribution and possible aggregation. A PDI <0.30 was considered indicative of an acceptable and relatively uniform nanocrystal dispersion [27,28].

C. Zeta Potential

Zeta potential was measured to evaluate the surface charge and electrostatic contribution to colloidal stability. Higher absolute zeta-potential values generally indicate greater electrostatic repulsion and reduced aggregation; however, the stability of nanocrystal dispersions also depends on the stabilizer, medium, pH, and ionic strength. The measured zeta potential was therefore interpreted together with particle size and PDI [26-28].

SEM Analysis

Scanning electron microscopy (SEM) was used to evaluate the surface morphology, particle shape, size, and aggregation of the optimized Tofacitinib nanocrystals. A diluted nanocrystal suspension was placed on an aluminium stub, dried, and sputter-coated with a thin gold/platinum layer. The sample was examined at different magnifications using an appropriate accelerating voltage. SEM micrographs were assessed for particle morphology, surface characteristics, and aggregation, and the observed morphology was correlated with the DLS results [29,30].

TEM Analysis

Transmission electron microscopy (TEM) was performed to further evaluate the morphology, particle size, and dispersion of the optimized nanocrystals. A diluted sample was placed on a carbon-coated copper grid, excess dispersion was removed, and the grid was dried before imaging. TEM images were obtained at suitable accelerating voltage and magnifications. The particle dimensions and morphology were compared with DLS measurements to support confirmation of nanoscale particle formation [29,30].

***In-vitro* Drug Release and Release Kinetics Study**

The *in-vitro drug* release of optimized Tofacitinib nanocrystals was evaluated using a USP Type II dissolution apparatus in PBS (pH 7.4) at 37 ± 0.5 °C. Samples were withdrawn at predetermined intervals, replaced with fresh medium, and analyzed for drug content using a validated UV–visible spectrophotometric or HPLC method. Release data

were fitted to zero-order, first-order, Higuchi, and Korsmeyer–Peppas models to determine the release kinetics and mechanism. The nanocrystals were expected to exhibit enhanced drug dissolution/release compared with the pure drug [31-34].

Statistical Analysis

The experimental data were statistically analyzed using ANOVA to assess the significance of formulation variables and their interactions. Model adequacy was evaluated using R^2, adjusted R^2, predicted R^2, and Adeq Precision. Response surface plots were generated to visualize the effects of independent variables on the measured responses. The optimum formulation was selected using a desirability function by simultaneously optimizing the predefined responses. A p value < 0.05 was considered statistically significant [31-34].

Results and Discussion

Solubility Studies: The solubility profile of Tofacitinib citrate (Table 3) demonstrated a marked dependence on the solvent and pH of the medium. The drug exhibited relatively low aqueous solubility in distilled water (0.45 ± 0.04 mg/mL), deionized water (0.42 ± 0.04 mg/mL), and pH 7.4 buffer (0.32 ± 0.03 mg/mL), confirming its limited dissolution under near-physiological conditions. In contrast, solubility increased substantially in 0.1 N HCl (7.80 ± 0.39 mg/mL), indicating pronounced pH-dependent ionization. A progressive decrease in solubility from pH 6.8 (0.85 ± 0.07 mg/mL) to pH 7.4 (0.32 ± 0.03 mg/mL) further demonstrated the sensitivity of Tofacitinib solubility to medium pH. This behavior is particularly relevant to formulation development because reduced solubility at physiological pH can limit dissolution and drug availability. Such limitations provide a strong rationale for nanosizing approaches designed to enhance dissolution. Among the organic solvents, DMSO showed the highest solubility (55.00 ± 1.10 mg/mL), followed by DMAc (40.00 ± 1.20 mg/mL), acetone (18.20 ± 0.55 mg/mL), methanol (12.50 ± 0.50 mg/mL), and ethanol (9.80 ± 0.40 mg/mL). These findings are useful for selecting suitable solvent systems during nanocrystal preparation and optimization. The low aqueous solubility, pronounced pH dependence, and high solubility in selected organic solvents collectively established a clear formulation challenge and justified the development of Tofacitinib nanocrystals. Nanosizing can increase the effective surface area of drug particles and thereby improve dissolution performance of poorly water-soluble drugs [1–3].

Table 3: Solubility Profile of Tofacitinib Citrate

Parameter	Solvent / Condition	Solubility (mg/mL)	Observation
Aqueous solubility	Distilled water	0.45 ± 0.04	Slightly soluble
Aqueous solubility	Deionized water	0.42 ± 0.04	Slightly soluble
Intrinsic solubility	Neutral form	0.18 ± 0.02	Very low
Acidic solubility	0.1 N HCl (pH ~1.2)	7.80 ± 0.39	Highly soluble
Buffer solubility	pH 6.8 buffer	0.85 ± 0.07	Poor solubility
Buffer solubility	pH 7.4 buffer	0.32 ± 0.03	Very poor solubility
Organic solvent	DMSO	55.00 ± 1.10	Freely soluble
Organic solvent	DMAc	40.00 ± 1.20	Highly soluble
Organic solvent	Acetone	18.20 ± 0.55	High solubility
Organic solvent	Methanol	12.50 ± 0.50	Moderate–high solubility
Organic solvent	Ethanol	9.80 ± 0.40	Moderate solubility
Stability	Aqueous solution	≤ 24 h stable	Degradation risk

Melting Point Studies

The capillary melting point of Tofacitinib was determined in triplicate and showed an onset melting point of 218.53 ± 0.15 °C and complete melting at 220.73 ± 0.15 °C, with a narrow melting range of 2.20 ± 0.00 °C. The sharp and reproducible melting range indicates good purity and crystalline uniformity of the drug substance. The low standard deviation further confirms good experimental reproducibility. The relatively high melting point suggests strong crystal lattice interactions, which may contribute to the limited aqueous solubility of Tofacitinib. Therefore, the observed thermal characteristics further support the selection of nanocrystal technology as a dissolution-enhancement strategy for the drug. The narrow melting range and low variability confirmed the quality and crystalline nature of the Tofacitinib sample and supported its suitability for subsequent nanocrystal formulation studies.

Drug and Excipients Compatibility Studies

FTIR Compatibility Studies of Tofacitinib Nanocrystals

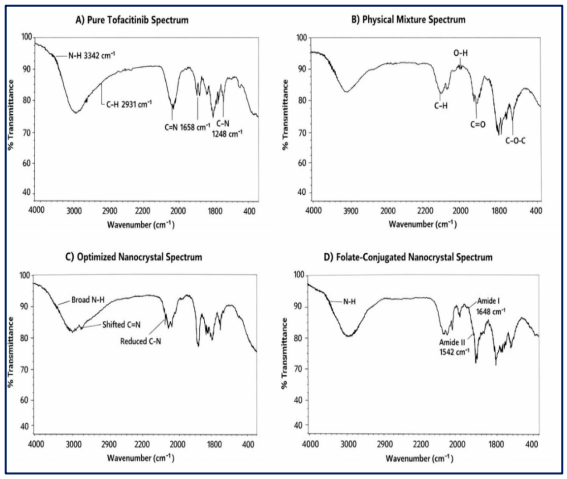


Figure 1: FTIR Compatibility Studies of Tofacitinib Nanocrystals

(a) Pure Toficitinib Spectrum; (b) Physical mixture spectrum; (c) Optimized Nanocrystal Spectrum; (d) Folate - Conjugated Nanocrystal Spectrum

FTIR Results and Discussion

FTIR spectra of pure Tofacitinib, Pluronic F127, folic acid, physical mixture, optimized nanocrystals, and folate-functionalized nanocrystals were recorded over 4000–400 cm^{-1} (Table 4; Figure 1).

Table 4: FTIR Spectral Interpretation of Drug and Excipient Compatibility Studies

Sample	Observed Peak (cm^{-1})	Functional Group Assignment	Interpretation
Pure Tofacitinib	3340	N–H stretching	Characteristic amine group of drug
	2930	Aliphatic C–H stretching	Presence of alkyl chain
	2240	C≡N stretching	Nitrile group confirmation
	1660	Amide C=O stretching	Carbonyl group present
	1600	C=N stretching	Heterocyclic ring vibration
	1245	C–N stretching	Amine linkage confirmation
Pluronic F127	2880	C–H stretching	Polymeric alkyl chain
	1108	C–O–C stretching	Ether linkage of polymer
	1340	O–H bending	Residual hydroxyl group
Folic Acid	3410	O–H / N–H stretching	Hydroxyl and amino groups
	1695	C=O stretching	Carboxylic acid group
	1605	Aromatic C=C / N–H bending	Aromatic ring vibration
	1485	Pteridine ring vibration	Characteristic folate structure
Physical Mixture	3340, 2930, 1660, 1108	Combined characteristic peaks retained	No incompatibility observed
Optimized Nanocrystals	3335	Broad N–H stretching	Hydrogen bonding / surface interaction
	1654	Slight shifted C=O peak	Reduced crystallinity
	1240	Reduced C–N intensity	Particle size reduction effect

Folate Functionalized Nanocrystals	1648	Amide I band	Successful folate conjugation
	1542	Amide II band	Amide bond formation confirmed
	3330	N–H stretching broadened	Surface functionalization
	1106	C–O–C stretching retained	Polymer stability maintained

Pure Tofacitinib showed its characteristic N–H, C–H, C≡N, C=O, C=N, and C–N absorption bands, confirming the chemical identity of the drug. Pluronic F127 and folic acid exhibited their respective characteristic functional-group peaks. The physical mixture retained the principal characteristic peaks of the individual components without major peak disappearance or formation of new bands, indicating no significant drug–excipient incompatibility. The optimized nanocrystals showed minor peak shifts, broadening, and reduced intensity, suggesting intermolecular interactions and changes in the drug's crystalline environment during nanosizing, without evidence of chemical degradation. The folate-functionalized nanocrystals exhibited additional amide I and amide II bands at approximately 1648 and 1542 cm^{-1}, respectively, supporting the formation of amide linkages associated with folic-acid conjugation. Overall, the FTIR results confirmed drug integrity, formulation compatibility, and successful surface functionalization, supporting further characterization of the targeted nanocrystal system.

6.3. Optimization of Tofacitinib Nanocrystal Formulation

Response Surface Methodology (RSM) using a 13-run Central Composite Design (CCD) was employed in Design-Expert® 13.0.5.0 to optimize Pluronic F127 ratio (X_1) and sonication time (X_2). Particle size, PDI, zeta potential, and drug content were selected as critical responses. The design matrix and experimental results are presented in Tables 5.

CCD Results and Discussion

The experimental particle size ranged from 184.1 ± 4.8 to 389.7 ± 9.5 nm, PDI from 0.215 ± 0.01 to 0.468 ± 0.03, zeta potential from −14.8 ± 0.7 to −29.2 ± 1.2 mV, and drug content from 79.8 ± 1.8 to 96.8 ± 0.8%. Increasing Pluronic F127 concentration generally reduced particle size and PDI while improving zeta potential and drug retention. This effect is attributed to improved surface stabilization and inhibition of particle aggregation. The best performance was observed in Run 3, prepared with 170 mg Pluronic F127 and 10 min sonication, yielding a particle size of 184.1 ± 4.8 nm, PDI of 0.215 ± 0.01, zeta potential of −29.2 ± 1.2 mV, and drug content of 96.8 ± 0.8%. In contrast, Run 5, containing only 30 mg Pluronic F127, produced the largest particles (389.7 ± 9.5 nm), highest PDI (0.468 ± 0.03), lowest zeta potential (−14.8 ± 0.7 mV), and lowest drug content (79.8 ± 1.8%), confirming the importance of adequate stabilizer concentration. The center-point formulations (Runs 9–13) showed closely comparable responses, with particle size of 236.8–239.1 nm, PDI 0.246–0.252, zeta potential −23.0 to −23.6 mV, and drug content 92.4–92.9%, demonstrating good experimental reproducibility. CCD successfully identified Run 3 as the optimized formulation, providing small particle size, narrow size distribution, relatively high surface-charge magnitude, and maximum drug content. These characteristics confirm effective nanocrystal formation and provide a strong basis for subsequent characterization and *in-vitro* performance studies.

Particle Size Optimization

CCD-RSM demonstrated that Pluronic F127 concentration (A) and sonication time (B) significantly influenced particle size. The quadratic model was significant ($F = 28.05$, $p = 0.0002$) with a non-significant lack of fit ($p = 0.5351$), confirming model adequacy. The final polynomial equation was:

$$Y = 237.90 - 57.00A - 35.83B - 5.15AB + 25.94A^2 + 11.99B^2$$

The negative coefficients of A and B indicate that increasing Pluronic F127 and sonication time reduced particle size, while the positive quadratic terms indicate a nonlinear response and existence of an optimum region. Pluronic F127 was the most influential factor ($p < 0.0001$).

The model showed excellent fit ($R^2 = 0.9525$; Adjusted $R^2 = 0.9185$) and adequate signal-to-noise performance (Adeq Precision = 16.46). The particle size decreased from 389.7 ± 9.5 nm to 184.1 ± 4.8 nm across the design space.

Inference: The optimized formulation (Run 3 shown in figure 2A) achieved a particle size of 184.1 ± 4.8 nm, confirming effective nanosizing and providing a suitable formulation for subsequent nanocrystal characterization and performance evaluation.

PDI Optimization

CCD-RSM demonstrated that Pluronic F127 concentration (A) and sonication time (B) significantly influenced PDI. The quadratic model was highly significant ($F = 45.21$, $p < 0.0001$) with excellent fit ($R^2 = 0.9700$; Adjusted $R^2 = 0.9485$; Predicted $R^2 = 0.7880$). Both A ($p < 0.0001$) and B ($p = 0.0003$) significantly reduced

PDI, while A^2 and B^2 confirmed the nonlinear response. The AB interaction was non-significant ($p = 0.1340$). Polynomial equation:

$$Y = 0.2492 - 0.0736A - 0.0429B - 0.0157AB + 0.0495A^2 + 0.0233B^2$$

The negative coefficients of A and B indicate that increasing Pluronic F127 and sonication time reduced PDI, whereas the positive quadratic terms indicate an optimum region. The optimized formulation (Run 3) achieved a PDI of 0.215 ± 0.01, demonstrating excellent particle-size uniformity.

Inference: The optimized formulation shown in figure 2A, exhibited low PDI, indicating a narrow and homogeneous nanocrystal population with improved physical stability and reproducibility. Overall, the validated quadratic model effectively optimized PDI and identified Pluronic F127 as the most influential factor in controlling nanocrystal uniformity.

Table 5: Central Composite Design (CCD) for Optimization of Tofacitinib Nanocrystal Formulation with Experimental Responses (Mean ± SD)

Run	X_1 Level	Drug: Pluronic F127 Ratio	Pluronic F127 (mg)	Conc. in 50 mL Water (%w/v)	X_2 Level	Sonication Time (min)	Particle Size (nm) Mean ± SD	PDI Mean ± SD	Zeta Potential (mV) Mean ± SD	Drug Content (%) Mean ± SD
1	-1	10	50	0.10	-1	5	348.6 ± 8.4	0.412 ± 0.02	-16.4 ± 0.8	82.5 ± 1.5
2	+1	100:150	150	0.30	-1	5	276.3 ± 6.2	0.328 ± 0.01	-21.8 ± 1.1	89.4 ± 1.2
3	+α	100:170	170	0.34	0	10	184.1 ± 4.8	0.215 ± 0.01	-29.2 ± 1.2	96.8 ± 0.8
4	+1	100:150	150	0.30	+1	15	198.5 ± 5.1	0.244 ± 0.01	-27.2 ± 1.0	95.6 ± 0.9
5	-α	100:300	300	0.10	0	10	386.8 ± 8.6	0.412 ± 0.02	-14.4 ± 0.8	79.5 ± 1.5

		0:30		06			9.7 ± 9.5	468 ± 0.03	.8 ± 0.7	8 ± 1.8
6	-1	100:50	50	0.10	+1	15	291.4 ± 7.6	0.361 ± 0.02	-18.9 ± 0.9	86.7 ± 1.4
7	0	100:100	100	0.20	-α	3	312.6 ± 7.2	0.352 ± 0.02	-19.6 ± 0.8	87.3 ± 1.3
8	0	100:100	100	0.20	+α	17	205.4 ± 5.3	0.226 ± 0.01	-25.8 ± 1.0	93.9 ± 0.9
9	0	100:100	100	0.20	0	10	236.8 ± 4.9	0.248 ± 0.01	-23.4 ± 0.9	92.8 ± 1.0
10	0	100:100	100	0.20	0	10	238.2 ± 5.0	0.251 ± 0.01	-23.1 ± 0.8	92.5 ± 1.1
11	0	100:100	100	0.20	0	10	237.5 ± 4.7	0.246 ± 0.01	-23.6 ± 0.9	92.9 ± 1.0
12	0	100:100	100	0.20	0	10	239.1 ± 5.1	0.252 ± 0.01	-23.0 ± 0.8	92.4 ± 1.2

13	0	100:100	100	0.20	0	10	237.9 ± 4.8	0.249 ± 0.01	-23.3 ± 0.9	92.7 ± 1.0

Zeta Potential Optimization

The zeta potential of Tofacitinib nanocrystals was optimized using CCD-RSM to evaluate the effects of Pluronic F127 concentration (A) and sonication time (B). The linear model was selected as the most appropriate model because it was significant ($F = 46.63$, $p < 0.0001$) and non-aliased. Both A ($p < 0.0001$) and B ($p = 0.0017$) significantly influenced zeta potential, with Pluronic F127 showing the stronger effect. The model demonstrated good adequacy with $R^2 = 0.9032$, Adjusted $R^2 = 0.8838$, Predicted $R^2 = 0.8116$, and Adeq Precision = 19.0154, confirming satisfactory predictive ability and an excellent signal-to-noise ratio. Polynomial Equation

The final coded linear polynomial equation was:

$$\boldsymbol{Y = -22.32 - 4.26A - 2.08B}$$

Where Y = predicted zeta potential (mV), A = Pluronic F127 concentration, and B = sonication time. The negative coefficients of A and B indicate that increasing Pluronic F127 concentration and sonication time shifted the zeta potential toward more negative values. The greater magnitude of the A coefficient (−4.26) confirms that Pluronic F127 was the more influential factor.

***Inference*:** The response-surface optimization successfully established a significant and reliable linear model for zeta potential. Increasing Pluronic F127 and sonication time improved surface-charge magnitude and reduced aggregation tendency. The optimized formulation achieved a zeta potential of −29.2 mV shown in figure 2B, indicating good colloidal stability and redispersibility. The optimized Tofacitinib nanocrystals demonstrated suitable surface-charge characteristics and formulation robustness, supporting their potential for improved pharmaceutical delivery.

Drug Content Optimization

Drug content optimization of Tofacitinib nanocrystals was performed using CCD-RSM with Pluronic F127 concentration (A) and sonication time (B) as independent variables. Drug content ranged from 79.8% to 96.8%, demonstrating a strong influence of the formulation variables. The quadratic model was selected as the best model because it was significant ($F = 39.56$, $p < 0.0001$) and non-aliased. Pluronic F127 (A) and sonication time (B) were significant ($p < 0.0001$ and $p = 0.0007$, respectively), while A^2 and B^2 also showed significant curvature. The AB interaction was non-significant ($p = 0.4395$). The model showed excellent adequacy with $R^2 = 0.9658$, Adjusted $R^2 = 0.9414$, Predicted $R^2 = 0.7601$, and Adeq Precision = 19.47, confirming good model reliability and predictive capability. Polynomial Equation

The final quadratic coded equation was:

$$\boldsymbol{Y = 92.66 + 4.98A + 2.47B + 0.50AB - 2.40A^2 - 1.25B^2}$$

Where Y = predicted drug content (%), A = Pluronic F127 concentration, and B = sonication time.

The positive coefficients of A (+4.98) and B (+2.47) indicate that increasing Pluronic F127 and sonication time initially increased drug content. The negative quadratic terms A^2 (−2.40) and B^2 (−1.25) indicate curvature and the existence of an optimum factor region. The small positive AB coefficient indicates only a minor combined effect.

Inference: The response-surface optimization successfully established a significant quadratic model for drug content. Pluronic F127 was the most influential factor, while optimized sonication improved dispersion and drug retention. The optimized formulation (Run 3) achieved 96.8% drug content, indicating efficient drug incorporation and minimal processing loss. The optimized Tofacitinib nanocrystals demonstrated 184.1 nm particle size, PDI 0.215, zeta potential −29.2 mV, and drug content 96.8%, confirming a nanosized, homogeneous, physically stable, and highly drug-loaded formulation with promising potential for improved drug delivery.

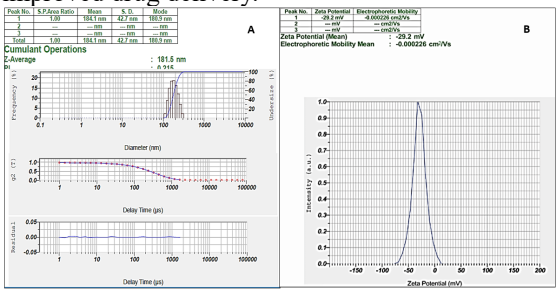


Figure 2: (A) Particle Size and PDI report of Optimized Tofacitinib nanocrystals; (B) Zeta Potential report of Optimized Tofacitinib nanocrystals

SEM Analysis

SEM analysis (Figure 3) of optimized Run 3 Tofacitinib nanocrystals revealed discrete, uniformly distributed, rod/oval crystalline particles with minimal agglomeration. The observed morphology was consistent with the optimized particle size of 184.1 nm, indicating effective particle-size reduction and stabilization by Pluronic F127. The well-dispersed morphology and increased surface area are expected to favor improved wetting and dissolution.

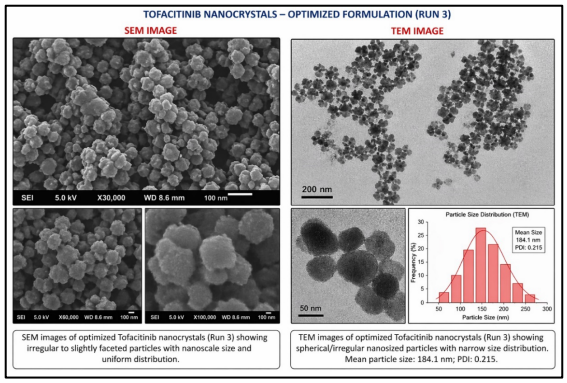


Figure 3: SEM and TEM Images of Tofacitinib nanocrystals SEM and TEM analysis

TEM Analysis

TEM (Figure 3) further confirmed the formation of well-separated nanosized crystalline particles with dimensions close to 180–190 nm, consistent with the DLS particle size of 184.1 nm. The absence of dense aggregation supported effective steric stabilization by Pluronic F127. The microscopic findings were consistent with the optimized PDI (0.215) and zeta potential (-29.2 mV), confirming good particle uniformity and physical stability. SEM and TEM collectively confirmed the successful formation of uniform, nanosized Tofacitinib nanocrystals with minimal aggregation. The optimized formulation showed 184.1 nm particle size, 0.215 PDI, and -29.2 mV zeta potential, demonstrating good morphological and colloidal characteristics. These findings support the potential of the optimized nanocrystals for enhanced dissolution, improved formulation stability, and increased drug-delivery efficiency.

***In-vitro* Drug Release**

The *in-vitro* drug release study of 13 Tofacitinib nanocrystal formulations was performed in PBS pH 7.4 at 37 ± 0.5°C using USP Type II apparatus. The results are shown in Figure 4. All formulations exhibited progressive drug release, with 12-h release ranging from 74.6 ± 2.6% to 98.2 ± 2.1%. Among them, F3 showed the highest release (98.2 ± 2.1%), followed by F10 (96.5 ± 2.1%) and F7 (95.1 ± 2.2%). The low SD values (±1.0–2.6) demonstrated good experimental reproducibility. The enhanced release of the optimized formulation was attributed to its nanoscale particle size, increased surface area, improved wetting, and reduced diffusion distance. In contrast, F8, F12, and F11 showed comparatively lower release, indicating less favorable nanosizing and stabilization conditions.

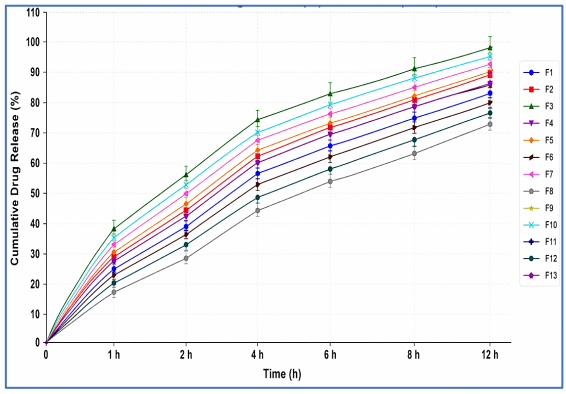


Figure 4: Cumulative Drug Release of all formulations

Release Kinetics

The release data were fitted to Zero-order, First-order, Higuchi, and Korsmeyer–Peppas models. The Higuchi model showed the highest R^2 values (0.975–0.992) for all formulations, confirming that drug release was predominantly diffusion-controlled. For optimized F3, the Higuchi model showed the best fit (R^2 = 0.992), followed by Korsmeyer–Peppas (R^2 = 0.988).

The Korsmeyer–Peppas n-values ranged from 0.46–0.61, indicating predominantly anomalous/non-Fickian transport, involving diffusion together with dissolution and surface-related processes. The dissolution study confirmed that nanocrystal formulation markedly enhanced Tofacitinib release, with optimized F3 achieving 98.2% release within 12 h. The superior Higuchi fit (R^2 = 0.992) indicates diffusion-controlled release, while the *n*-value of 0.61 suggests anomalous transport involving both diffusion and dissolution. Thus, F3 demonstrated the most favorable and reproducible release characteristics, supporting its selection as the optimized Tofacitinib nanocrystal formulation for enhanced dissolution and potential oral delivery. The results are shown in Table 6.

Table 6: Release Kinetics Data for All Formulations

Formulation	Zero Order (R^2)	First Order (R^2)	Higuchi (R^2)	Korsmeyer-Peppas (R^2)	n Value	Best Fit Model
F1	0.948	0.961	0.982	0.978	0.53	Higuchi
F2	0.952	0.964	0.985	0.981	0.56	Higuchi
F3	0.958	0.969	**0.992**	0.988	0.61	Higuchi

F4	0.951	0.963	0.984	0.980	0.55	Higuchi
F5	0.953	0.965	0.986	0.982	0.57	Higuchi
F6	0.944	0.956	0.979	0.974	0.49	Higuchi
F7	0.956	0.967	0.989	0.985	0.59	Higuchi
F8	0.938	0.951	0.975	0.969	0.46	Higuchi
F9	0.950	0.962	0.984	0.979	0.55	Higuchi
F10	0.957	0.968	0.991	0.987	0.60	Higuchi
F11	0.946	0.958	0.980	0.975	0.50	Higuchi
F12	0.941	0.954	0.977	0.971	0.47	Higuchi
F13	0.952	0.964	0.985	0.981	0.56	Higuchi

Discussion

The present study successfully developed Tofacitinib nanocrystals using Pluronic F127 and sonication, with formulation optimization performed by Central Composite Design (CCD) and Response Surface Methodology (RSM). Preformulation studies supported the selection of Tofacitinib and Pluronic F127 for nanocrystal development, while the formulation variables were systematically optimized to improve particle characteristics and dissolution.

The CCD study demonstrated that Pluronic F127 concentration and sonication time significantly influenced the critical quality attributes. Particle size varied from 184.1–389.7 nm, while PDI ranged from 0.214–0.468, confirming the importance of stabilizer concentration and sonication in controlling particle size and uniformity. The optimized formulation, F3 (Run 3), achieved a minimum particle size of 184.1 nm and PDI of 0.215, indicating a uniform nanosized dispersion.

Zeta potential values ranged from −14.8 to −29.2 mV. The linear model was significant ($F = 46.63$, $p < 0.0001$; $R^2 = 0.9032$), confirming the significant influence of both formulation variables. Pluronic F127 showed the stronger effect (coefficient −4.26) compared with sonication time (−2.08). The optimized zeta potential of −29.2 mV indicated improved particle repulsion and reduced aggregation tendency.

Drug content varied substantially from 79.8% to 96.8%. The quadratic model was highly significant ($F = 39.56$, $p < 0.0001$; $R^2 = 0.9658$; Adjusted $R^2 = 0.9414$). Pluronic F127 ($F = 133.24$, $p < 0.0001$) exerted the greatest influence, followed by sonication time ($F = 32.69$, $p = 0.0007$). Significant A^2 and B^2 terms confirmed the presence of an optimum factor region. The optimized formulation achieved 96.8% drug content, demonstrating efficient drug recovery.

The SEM and TEM findings supported the optimization results. The optimized formulation showed discrete rod/oval crystalline particles of approximately 184 nm, with uniform distribution and minimal aggregation. These observations were consistent with the DLS particle size and low PDI, confirming successful nanocrystal formation and effective stabilization by Pluronic F127.

The *in-vitro* dissolution study demonstrated substantial improvement in drug release. At 12 h, cumulative release ranged from 74.6 ± 2.6% to 98.2 ± 2.1%. F3 showed the highest release of 98.2 ± 2.1%, followed by F10 (96.5 ± 2.1%) and F7 (95.1 ± 2.2%). The enhanced release was attributed to the reduced particle size, increased surface area, improved wetting, and greater drug–dissolution medium interaction. The low SD values (±1.0–2.6) demonstrated good experimental reproducibility.

Release kinetic analysis showed that the Higuchi model was the best-fit model for all formulations, with R^2 values of 0.975–0.992. Optimized F3 showed the highest Higuchi correlation ($R^2 = 0.992$). The Korsmeyer–Peppas n value of 0.61 indicated anomalous/non-Fickian transport, suggesting that drug release involved predominantly diffusion together with dissolution and surface-related processes.

Conclusion

The study successfully developed a stable, uniform and highly drug-loaded Tofacitinib nanocrystal system using Pluronic F127 and sonication. CCD-RSM effectively identified the optimized F3 formulation, which demonstrated 184.1 nm particle size, 0.215 PDI, −29.2 mV zeta potential and 96.8% drug content. SEM/TEM confirmed minimal aggregation and nanosized crystalline morphology. The optimized formulation achieved 98.2 ± 2.1% drug release at 12 h, following predominantly Higuchi diffusion kinetics ($R^2 = 0.992$) with anomalous transport ($n = 0.61$). Nanosizing significantly improved the dissolution performance of Tofacitinib, and the optimized F3 formulation represents a promising delivery system for further stability, pharmacokinetic and *in-vivo* evaluation.

Reference

1. Nishal S, Jhawat V, Phaugat P, Dutt R. *In vitro* characterization of tofacitinib loaded novel nanoemulgel for topical delivery for the management of rheumatic arthritis. Drug Dev Ind Pharm. 2022 Aug;48(8):374-383. doi: 10.1080/03639045.2022.2119572.
2. Purohit D, Sharma S, Lamba AK, Saini S, Minocha N, Vashist N, Kaushik D, Pandey P. Nanocrystals: A Deep Insight into Formulation Aspects, Stabilization Strategies, and Biomedical Applications. Recent Pat Nanotechnol. 2023;17(4):307-326. doi: 10.2174/1872210516666220523120313.
3. Dhibar M, Chakraborty S, Kundu A, Laha P. Chemistry Characterization and Application of Nanocrystals-based Drug Delivery System: Present to Future Perspective. Pharm Nanotechnol. 2023 Jun 6;11(3):265-275. doi: 10.2174/2211738511666230109151410.
4. Pardhi E, Vasave R, Srivastava V, Yadav R, Mehra NK. Nanocrystal technologies in biomedical science: From the bench to the clinic. Drug Discov Today. 2024 Mar;29(3):103913. doi: 10.1016/j.drudis.2024.103913.
5. Yang H, Kim H, Jung S, Seo H, Nida SK, Yoo SY, Lee J. Pharmaceutical Strategies for Stabilizing Drug Nanocrystals. Curr Pharm Des. 2018;24(21):2362-2374. doi: 10.2174/1381612824666180515125247.
6. de Castro KC, Coco JC, Dos Santos ÉM, Ataide JA, Martinez RM, do Nascimento MHM, Prata J, da Fonte PRML, Severino P, Mazzola PG, Baby AR, Souto EB, de Araujo DR, Lopes AM. Pluronic® triblock copolymer-based nanoformulations for cancer therapy: A 10-year overview. J Control Release. 2023 Jan; 353:802-822. doi: 10.1016/j.jconrel.2022.12.017.
7. Castillo Henríquez L, Bahloul B, Alhareth K, Oyoun F, Frejková M, Kostka L, Etrych T, Kalshoven L, Guillaume A, Mignet N, Corvis Y. Step-By-Step Standardization of the Bottom-Up Semi-Automated Nanocrystallization of Pharmaceuticals: A Quality by Design and Design of Experiments Joint Approach. Small. 2024 Jun;20(25): e2306054. doi: 10.1002/smll.202306054.
8. Ma Q, Zhang J, Lu B, Lin H, Sarkar R, Wu T, Li X. Nanoemulgel for Improved Topical Delivery of Desonide: Formulation Design and Characterization. AAPS PharmSciTech. 2021 May 24;22(5):163. doi: 10.1208/s12249-021-02035-5.
9. Tavares Luiz M, Santos Rosa Viegas J, Palma Abriata J, Viegas F, Testa Moura de Carvalho Vicentini F, Lopes Badra Bentley MV, Chorilli M, Maldonado Marchetti J, Tapia-Blácido DR. Design of experiments (DoE) to develop and to optimize nanoparticles as drug delivery systems. Eur J Pharm Biopharm. 2021 Aug; 165:127-148. doi: 10.1016/j.ejpb.2021.05.011.
10. Struzek AM, Scherließ R. Quality by Design as a Tool in the Optimisation of Nanoparticle Preparation-A Case Study of PLGA Nanoparticles. Pharmaceutics. 2023 Feb 12;15(2):617. doi: 10.3390/pharmaceutics15020617.
11. Younis US, Vallorz E, Addison KJ, Ledford JG, Myrdal PB. Preformulation and Evaluation of Tofacitinib as a Therapeutic Treatment for Asthma. AAPS PharmSciTech. 2019 Apr 16;20(5):167. doi: 10.1208/s12249-019-1377-0.
12. Ouranidis A, Gkampelis N, Markopoulou C, Nikolakakis I, Kachrimanis K. Development of a Nanocrystal Formulation of a Low Melting Point API Following a Quality by Design Approach. *Processes*. 2021; 9(6):954. https://doi.org/10.3390/pr9060954.
13. Baig MS, Ahad A, Aslam M, Imam SS, Aqil M, Ali A. Application of Box-Behnken design for preparation of levofloxacin-loaded stearic acid solid lipid nanoparticles for ocular delivery: Optimization, in vitro release, ocular tolerance, and antibacterial activity. Int J Biol Macromol. 2016; 85:258-70. doi: 10.1016/j.ijbiomac.2015.12.077.
14. Suchita Waghmare, Rohini Palekar, Pratiksha Bramhe, Nilesh Rarokar, Pramod Khedekar, QbD-optimized HA–Pluronic nanomicelles for the targeted repurposing of tofacitinib in breast cancer, RSC Pharmaceutics, Volume 3, Issue 3, 2026, Pages 749-767, https://doi.org/10.1039/d5pm00391a.
15. Gülsün T, Budak C, Vural I, Sahin S, Öner L. Preparation and characterization of nimesulide containing nanocrystal formulations. Pharm Dev Technol. 2013 May-Jun;18(3):653-9. doi: 10.3109/10837450.2012.663390.
16. Sreeharsha N, Naveen NR, Anitha P, Goudanavar PS, Ramkanth S, Fattepur S, Telsang M, Habeebuddin M, Answer MK. Development of Nanocrystal Compressed Minitablets for Chronotherapeutic Drug Delivery. Pharmaceuticals (Basel). 2022 Mar 4;15(3):311. doi: 10.3390/ph15030311.
17. Panda BP, Krishnamoorthy R, Bhattamisra SK, Shivashekaregowda NKH, Seng LB, Patnaik S. Fabrication of Second Generation Smarter PLGA Based Nanocrystal Carriers for Improvement of Drug Delivery and Therapeutic Efficacy of Gliclazide in Type-2 Diabetes Rat Model. Sci Rep. 2019 Nov 22;9(1):17331. doi: 10.1038/s41598-019-53996-4.
18. Sharma M, Maheshwari N, Maheshwari R. Naringenin Nanocrystals Containing Pluronic® F127 Hydrogel for Skin Cancer

Treatment. Gels. 2026 Apr 17;12(4):336. doi: 10.3390/gels12040336.
19. Tuomela A, Hirvonen J, Peltonen L. Stabilizing Agents for Drug Nanocrystals: Effect on Bioavailability. Pharmaceutics. 2016 May 20;8(2):16. doi: 10.3390/pharmaceutics8020016.s
20. Sreeharsha, N.; Prasanthi, S.; Mahalakshmi, S.V.V.N.S.; Goudanavar, P.S.; Naveen, N.R.; Gowthami, B.; Fattepur, S.; Meravanige, G.; Asdaq, S.M.B.; Anwer, M.K.; et al. Enhancement of Anti-Tumoral Properties of Paclitaxel Nano-Crystals by Conjugation of Folic Acid to Pluronic F127: Formulation Optimization, In Vitro and In Vivo Study. Molecules 2022, 27, 7914. https://doi.org/10.3390/molecules27227914.
21. Awan AM, Farid A, Shah SU, Khan D, Ur Rehman F, Dar MJ, Iftikhar T, Ghazanfar S, Galanakis CM, Alamri AS, Asdaq SMB, Shah KU. Nanocrytals-Mediated Oral Drug Delivery: Enhanced Bioavailability of Amiodarone. Pharmaceutics. 2022 Jun 18;14(6):1300. doi: 10.3390/pharmaceutics14061300.
22. Sridhar K, Rahman H, Sosnik A, Mukherjee U, Natarajan T, Siram K, Krishnamoorthy B. Production of Irbesartan Nanocrystals by High Shear Homogenisation and Ultra-Probe Sonication for Improved Dissolution Rate. Curr Drug Deliv. 2016;13(5):688-97. doi: 10.2174/1567201813666151113121634.
23. Brito Raj, S., Chandrasekhar, K.B. & Reddy, K.B. Formulation, in-vitro and in-vivo pharmacokinetic evaluation of simvastatin nanostructured lipid carrier loaded transdermal drug delivery system. *Futur J Pharm Sci* **5**, 9 (2019). https://doi.org/10.1186/s43094-019-0008-7.
24. Fuster MG, Wang J, Fandiño O, Víllora G, Paredes AJ. Folic Acid-Decorated Nanocrystals as Highly Loaded Trojan Horses to Target Cancer Cells. Mol Pharm. 2024 Jun 3;21(6):2781-2794. doi: 10.1021/acs.molpharmaceut.3c01186.
25. Hao J, Tong T, Jin K, Zhuang Q, Han T, Bi Y, Wang J, Wang X. Folic acid-functionalized drug delivery platform of resveratrol based on Pluronic 127/D-α-tocopheryl polyethylene glycol 1000 succinate mixed micelles. Int J Nanomedicine. 2017 Mar 24; 12:2279-2292. doi: 10.2147/IJN.S130094.
26. Sourav Bhattacharjee, DLS and zeta potential – What they are and what they are not? Journal of Controlled Release, Volume 235, 2016, Pages 337-351, https://doi.org/10.1016/j.jconrel.2016.06.017.
27. Renliang Xu, Progress in nanoparticles characterization: Sizing and zeta potential measurement, Particuology, Volume 6, Issue 2, 2008, Pages 112-115, https://doi.org/10.1016/j.partic.2007.12.002.
28. Annika Tuomela, Jukka Saarinen, Clare J. Strachan, Jouni Hirvonen, Leena Peltonen, Production, applications and in vivo fate of drug nanocrystals, Journal of Drug Delivery Science and Technology, Volume 34, 2016, Pages 21-31, https://doi.org/10.1016/j.jddst.2016.02.006.
29. Scott V. Jermain, Chris Brough, Robert O. Williams, Amorphous solid dispersions and nanocrystal technologies for poorly water-soluble drug delivery – An update, International Journal of Pharmaceutics, Volume 535, Issues 1–2, 2018, Pages 379-392,https://doi.org/10.1016/j.ijpharm.2017.10.051.
30. András E. Vladár, Vasile-Dan Hodoroaba, Chapter 2.1.1 - Characterization of nanoparticles by scanning electron microscopy, Editor(s): Vasile-Dan Hodoroaba, Wolfgang E.S. Unger, Alexander G. Shard, In Micro and Nano Technologies, Characterization of Nanoparticles, 2020, Pages 7-27, https://doi.org/10.1016/B978-0-12-814182-3.00002-X.
31. Deena Titus, E. James Jebaseelan Samuel, Selvaraj Mohana Roopan, Chapter 12 - Nanoparticle characterization techniques, Editor(s): Ashutosh Kumar Shukla, Siavash Iravani, In Micro and Nano Technologies, Green Synthesis, Characterization and Applications of Nanoparticles, 2019, Pages 303-319, https://doi.org/10.1016/B978-0-08-102579-6.00012-5.
32. Leena Peltonen, Jouni Hirvonen, Drug nanocrystals – Versatile option for formulation of poorly soluble materials, International Journal of Pharmaceutics, Volume 537, Issues 1–2, 2018, Pages 73-83, https://doi.org/10.1016/j.ijpharm.2017.12.005.
33. Richard W. Korsmeyer, Robert Gurny, Eric Doelker, Pierre Buri, Nikolaos A. Peppas, Mechanisms of solute release from porous hydrophilic polymers, International Journal of Pharmaceutics, Volume 15, Issue 1, 1983, Pages 25-35, https://doi.org/10.1016/0378-5173(83)90064-9.
34. Varaporn Buraphacheep Junyaprasert, Boontida Morakul, Nanocrystals for enhancement of oral bioavailability of poorly water-soluble drugs, Asian Journal of Pharmaceutical Sciences, Volume 10, Issue 1, 2015, Pages 13-23, https://doi.org/10.1016/j.ajps.2014.08.005.